

# STM-induced reversible switching of local conductivity in thin Al<sub>2</sub>O<sub>3</sub> films

**Citation for published version (APA):**

Kurnosikov, O., Nooij, de, F. C., LeClair, P. R., Kohlhepp, J. T., Koopmans, B., Swagten, H. J. M., & Jonge, de, W. J. M. (2001). STM-induced reversible switching of local conductivity in thin Al<sub>2</sub>O<sub>3</sub> films. *Physical Review B*, 64(15), 153407-1/4. [153407]. <https://doi.org/10.1103/PhysRevB.64.153407>, <https://doi.org/10.1103/PhysRevB.64.153407>

**DOI:**

[10.1103/PhysRevB.64.153407](https://doi.org/10.1103/PhysRevB.64.153407)  
[10.1103/PhysRevB.64.153407](https://doi.org/10.1103/PhysRevB.64.153407)

**Document status and date:**

Published: 01/01/2001

**Document Version:**

Publisher's PDF, also known as Version of Record (includes final page, issue and volume numbers)

**Please check the document version of this publication:**

- A submitted manuscript is the version of the article upon submission and before peer-review. There can be important differences between the submitted version and the official published version of record. People interested in the research are advised to contact the author for the final version of the publication, or visit the DOI to the publisher's website.
- The final author version and the galley proof are versions of the publication after peer review.
- The final published version features the final layout of the paper including the volume, issue and page numbers.

[Link to publication](#)

**General rights**

Copyright and moral rights for the publications made accessible in the public portal are retained by the authors and/or other copyright owners and it is a condition of accessing publications that users recognise and abide by the legal requirements associated with these rights.

- Users may download and print one copy of any publication from the public portal for the purpose of private study or research.
- You may not further distribute the material or use it for any profit-making activity or commercial gain
- You may freely distribute the URL identifying the publication in the public portal.

If the publication is distributed under the terms of Article 25fa of the Dutch Copyright Act, indicated by the "Taverne" license above, please follow below link for the End User Agreement:

[www.tue.nl/taverne](http://www.tue.nl/taverne)

**Take down policy**

If you believe that this document breaches copyright please contact us at:

[openaccess@tue.nl](mailto:openaccess@tue.nl)

providing details and we will investigate your claim.

## STM-induced reversible switching of local conductivity in thin Al<sub>2</sub>O<sub>3</sub> films

O. Kurnosikov, F. C. de Nooij, P. LeClair, J. T. Kohlhepp, B. Koopmans, H. J. M. Swagten, and W. J. M. de Jonge  
 Eindhoven University of Technology, Department of Applied Physics and COBRA Research Institute, P.O. Box 513, 5600 MB, Eindhoven,  
 The Netherlands

(Received 15 February 2001; revised manuscript received 18 May 2001; published 18 September 2001)

The local electron transport properties of thin aluminum oxide layers used for magnetic tunnel junctions were studied *in situ* by scanning tunneling microscopy (STM) and spectroscopy under ultrahigh-vacuum conditions. The STM images of the oxide films reveal a granular structure, down to atomic resolution. A reversible switching of the conductive properties of grains, attributed to a charge redistribution, is observed during scanning. We demonstrate the possibility of intentionally switching a grain to the low-resistance state by exposing it to a high current density. We conjecture that the observed switching behavior may be considered as the precursor of an electric breakdown in tunnel junctions.

DOI: 10.1103/PhysRevB.64.153407

PACS number(s): 85.30.Mn, 73.40.Gk, 73.40.Rw, 85.70.Kh

Some of the most elementary properties of metal-insulator and semiconductor-insulator electronic devices have their origin at the subnanometer level. In particular phenomena related to quantum-mechanical tunneling and dielectric breakdown are extremely sensitive to atomic- or nanometer-sized details, such as the presence of defects at interfaces or in the insulator, interface roughness, and nanoscopic electrical shorts (pinholes). Many of the related fascinating phenomena are only poorly understood and require more detailed investigations of the local current transport at ultimate spatial resolution by means of scanning probe microscopy. Apart from their fundamental interest, these studies are generally considered to be of importance for progress in device technology. Dielectric breakdown is an important issue in the field of SiO<sub>2</sub>-based metal-oxide-semiconductor (MOS) devices,<sup>1</sup> in which because of miniaturization the oxide thickness will soon reach the nanometer level. For further development of magnetic tunnel junctions (MTJ's) for field sensor and data storage applications, inhomogeneous current distribution effects as well as breakdown are current matters of concern.<sup>2,3</sup> At present, Al<sub>2</sub>O<sub>3</sub> is the most widely used material for the ultrathin (~1 nm) barrier in MTJ's.

Recently, a number of studies on the local characterization and manipulation of electron transport in Al<sub>2</sub>O<sub>3</sub> (Refs. 4 and 5) and SiO<sub>2</sub> (Refs. 6 and 7) ultrathin films have been performed employing scanning tunneling microscopy<sup>5-7</sup> (STM) and atomic force microscopy (AFM) with a conductive cantilever.<sup>4</sup> As expected from the exponential dependence of the tunnel current on the width and height of the potential barrier, a strongly inhomogeneous distribution of the tunnel current has been observed.<sup>4</sup> More interestingly, it was found that applying a positive sample bias (electrons from tip to sample) of several volts leads to the *irreversible* formation of spots with an enhanced local conductivity.<sup>7</sup> In the more severe cases, large regions with a diameter of tens of nanometers and linear (metallic) current-voltage (*I-V*) characteristics were created.<sup>4</sup> In some of the studies smaller, *though irreversible*, leakage sites were induced that displayed non-metallic transport properties.<sup>6</sup> These phenomena can be distinguished as hard and soft breakdown, respectively.

In this paper, we report on more subtly induced effects in the local conductivity of amorphous Al<sub>2</sub>O<sub>3</sub> barriers. While

we also observed hard breakdown in some of our experiments, the present work addresses the creation and characterization of *reversible* switching of the local conductivity, which can be considered as a precursor of soft breakdown. Under proper conditions, a resolution down to the atomic length scale has been achieved, which guarantees correct STM operation. In order to resolve the electronic origin of the observed behavior and discriminate between topological and electronic effects we performed scanning tunneling spectroscopy (STS) in several configurations.

Samples were prepared by a procedure similar to the one used for production of MTJ's, which typically display a room-temperature magnetoresistance of 30% (Ref. 8) for pure Co electrodes. However, for the present experiments the preparation was interrupted before deposition of the top electrode to allow for local transport measurements. The bottom electrode of cobalt was deposited on a Ta buffer layer on oxidized Si substrates using UHV dc-magnetron sputtering at an argon pressure of  $7 \times 10^{-3}$  mbar. Al layers with thicknesses ranging from 0.5 to 2.5 nm were sputtered on top of the Co electrode. Finally, Al<sub>2</sub>O<sub>3</sub> was obtained by oxidation of the Al in an oxygen plasma at a pressure of 0.1 mbar, monitored optically to ensure proper oxidation.<sup>9</sup> Alternatively, for some of our thinnest films we used a "preoxidation" procedure: The topmost layers of the Co electrode were thermally oxidized prior to deposition of the Al. The more reactive Al was then spontaneously oxidized by scavenging the oxygen from the CoO. Independent of preparation, the oxidation of the aluminum layer as well as the absence of CoO<sub>x</sub> and chemisorbed oxygen was verified by x-ray photoemission spectroscopy.<sup>9</sup> For complete oxidation the thickness of the Al<sub>2</sub>O<sub>3</sub> film is estimated by multiplying the Al layer thickness by a factor of 1.3, yielding a thickness range from 0.7 to 3.3 nm. The samples were transferred to an Omicron STM-1 under UHV conditions. Electrochemically etched tungsten tips were used for the STM investigations. In all the experiments we applied a positive sample bias (electrons from tip to sample) over the sample.

Before presenting our data it is worthwhile elucidating some of the different regimes that can be met when performing STM on insulating thin films. At a bias voltage (*V*) below the barrier height of the insulator (*V<sub>B</sub>*, defined as the energy

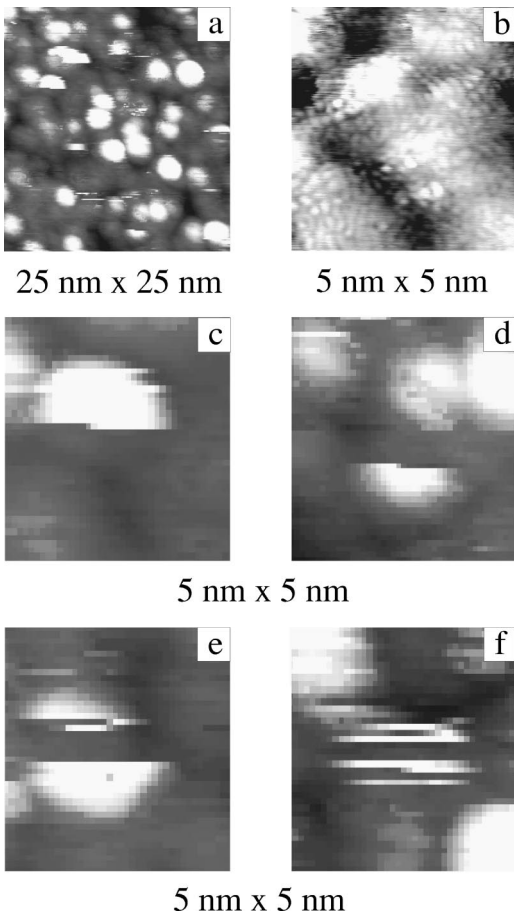


FIG. 1. STM images (constant current mode) of  $\text{Al}_2\text{O}_3$  thin films: (a) Overview at 2.23 V, 0.14 nA, and  $d_{ox}=0.8$  nm. (b) Atomic resolution on a  $d_{ox}=1.3$  nm film at 0.03 V and 13 nA. (c)–(f) Selected areas from panel (a), showing creation (c), annihilation (d), and instability of leakage sites (e), (f).

difference between the bottom of the conduction band and the Fermi level) current can only flow by tunneling through the insulator, whereas at higher bias ( $V > V_B$ ) electrons can also tunnel directly to the conducting band of the insulator. For even higher applied voltage above the work function ( $V > \Phi$ ) field emission may set in. As to the lowest-bias regime ( $V < V_B$ ) a simple order of magnitude estimate can be made of the STM current  $I$ . Within the WKB approximation in the low-bias limit and approximating the complex tip-sample configuration by a planar junction with an area  $A$  of atomic dimension, one finds  $I = e/h(A/d_{ox}^2)V_B^{1/2}V \exp(-2d_{ox}\sqrt{2mV_B/\hbar})$ . For our thinnest oxide layers,  $d_{ox} \sim 0.7$  nm, assuming the tip to be almost in contact with the film, and substitution of  $V_B \sim 1$  V,  $V \sim 0.1$  V, and  $A \sim 10^{-19}$  m<sup>2</sup> yields a current  $I \sim 1$  nA. For the thicker oxides ( $\geq 2$  nm) immeasurably small currents ( $< 10^{-15}$  A) are predicted in this low-bias regime.

Figure 1 represents STM images of the oxidized Al films. In Fig. 1(a) a grainlike structure of the aluminum oxide film is revealed, consisting of randomly distributed spots with a diameter of 1–3 nm. In this paper we will show that the granular structure after oxidation cannot entirely be associated with the morphology but is strongly influenced by local

variations in the electrical conductivity as well. It was verified that phenomena described in this paper are specific for the  $\text{Al}_2\text{O}_3$  films by comparing with STM characterization prior to oxidation and on the bare Co electrode.

For all but the thinnest oxide films, proper images were obtained with a positive bias voltage in the range 1.5–5 V, i.e.,  $V > V_B$ . However, for the thinner films ( $\leq 1.3$  nm) stable images were obtainable down to  $\sim 20$  mV. Under these conditions an atomic structure as shown in Fig. 1(b) was sometimes resolved. The rather disordered atomic arrangement is characterized by an average interatomic distance of 0.26 nm. This distance is in reasonable agreement with typical O-O distances in various  $\text{AlO}_x$  phases. This would support an interpretation of the atomic features in terms of the oxide surface atoms, which even for energies within the  $\text{Al}_2\text{O}_3$  band gap are weakly hybridized with the metallic wave functions of the Co electrode. Irrespective of the detailed interpretation, the atomic resolution serves as a proof of the good quality of the STM tip and the experimental setup in the present study.

While scanning at a high bias (1.5–5 V) and high current ( $> 1$  nA), the grainlike structure is found to display a rich dynamical behavior. Figures 1(a) and 1(c)–1(f) show detailed examples of the appearance and disappearance of bright spots with a diameter of  $\sim 3$  nm. Closer inspection of the images demonstrates that these features cannot be due to morphological changes or exchange of atoms between tip and sample. As an example, in Fig. 1(e) a spot appears exactly at the position where it disappeared before, and Fig. 1(f) represents a local area that displays a very instable behavior which can be associated with numerous irregular processes of switching on and off. These repeatable processes cannot be due to an instability of the STM tip, because outside the region of the spot the scanned lines are not affected. Most likely, the dynamical phenomena in the STM images correspond to a reaction of the feedback of the STM on sudden changes of local conductivity of the aluminum oxide film. Thus, the sudden increase or decrease in the apparent height by 0.5–1 nm corresponds to the switching on or off, respectively, of a local channel of enhanced conductivity, further on denoted as the “leakage site.” Analysis of a large number of features has shown that the creation of such a site is usually an STM-induced effect. This is concluded from the fact that it occurs most frequently right underneath the tip; i.e., a sudden change in brightness is observed while the tip is at the center of the leakage site [see, e.g., Fig. 1(c)].

Although in the experiments discussed so far the switching occurs at nonselected sites during scanning, Fig. 2 demonstrates the potential to switch a leakage site intentionally. The bottom half of Fig. 2(a) displays the first part of a scan. Then, at a site with relatively low conductance at the center of the image (indicated by the cross), the feedback current is ramped up to 4 nA. The STM responds by gradually reducing the tip-sample distance in order to provide the demanded current, as indicated in Fig. 2(d). Upon opening higher-conductance channels, sudden positive jumps occur. The dashed lines in the figure schematically illustrate the  $\Delta z$ - $I$  dependence expected in the absence of such discontinuities. A dramatic switching event is observed at 3.3 nA. When

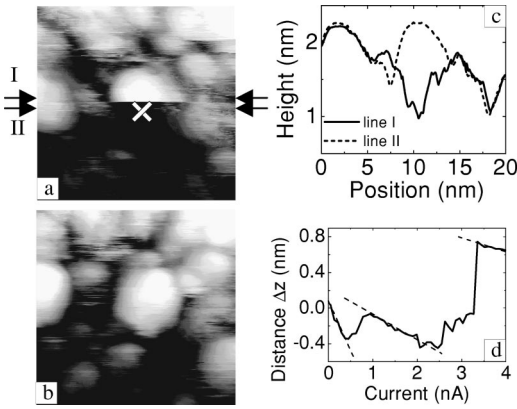


FIG. 2. Intentional creation of a leakage site in a  $d_{ox}=0.9$  nm film at 2.7 V. (a)  $20 \times 20$  nm<sup>2</sup> STM image at 0.082 nA before (bottom half) and after (top) ramping the current at the center of the image. (b) Image of the same area made 2 min after the ramping experiment. (c) Cross sections along lines indicated in (a). (d) Displacement of the tip while ramping the feedback current. The dashed lines indicate partial traces during which no instabilities occur.

scanning is continued [top part of Fig. 2(a)] it is seen that this event was accompanied by the creation of a leakage site, which is stable at least until the next image is scanned [Fig. 2(b)]. The two cross sections in Fig. 2(c) reveal an apparent height of the channel of  $\sim 1$  nm, i.e., equal to the abrupt withdrawal of the tip in the ramping experiment. These cross sections also illustrate that the conductivity in regions surrounding the switched channel is not affected.

At this stage we conclude that reversible and irreversible changes in the oxide conductance can be induced by driving a high current density through the oxide at a positive bias of several volts. In order to resolve the underlying electronic phenomena we performed  $I$ - $V$  and  $I$ - $z$  (current-distance) STS.<sup>10,11</sup> In interpreting STS on a complex barrier, consisting of an oxide layer in series with a vacuum gap, one has to realize that the voltage drop associated with the applied bias ( $V$ ) will be divided over the oxide ( $V_O$ ) and the vacuum gap ( $V_V = V - V_O$ ). In general, polarization of the dielectric film tends to reduce the potential of the oxide-vacuum interface, while accumulation of electrons (at positive bias) has an opposite effect. For a more quantitative description, detailed knowledge of the dielectric properties, charge trapping sites, and exact shape of the STM tip is required.

Some results of  $I$ - $V$  spectroscopy are presented in Fig. 3. Because of the occurrence of induced switching effects at high current, relatively stable  $I$ - $V$  curves could be measured only at low current,  $I < 100$  pA. An example of  $I$ - $V$  averaged over several tip positions is presented in the inset of Fig. 3(a). We limit our analysis to the more stable positive-bias regime for which electrons tunnel from the tip to the sample. On a logarithmic scale, two almost linear regimes can be recognized in the spectrum with a transition to a lower slope at  $V_c = 2.6$  V. Modeling of the tunneling through the oxidic and vacuum barrier in series indicates that  $V_c$  should be associated with  $V_B + V_O$ . For realistic parameters one thus obtains an estimate  $V_B \sim 1-2$  V. This can be

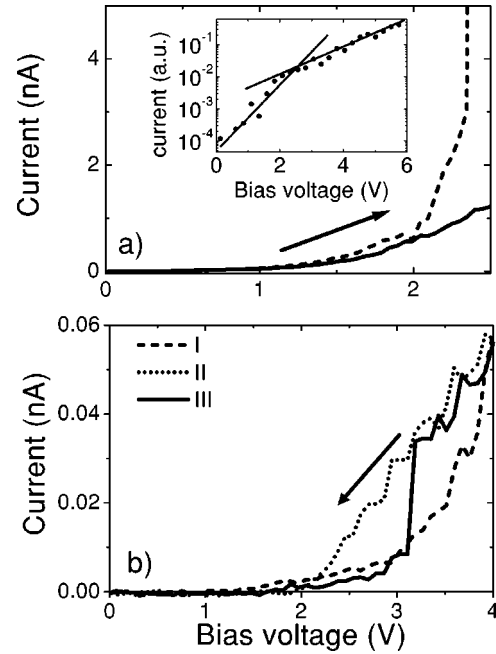


FIG. 3.  $I$ - $V$  spectroscopy at various distances. Inset:  $I$ - $V$  measured at a low current of 0.1 nA,  $d_{ox}=1.4$  nm. (a) Two  $I$ - $V$  curves (dashed, solid lines) at a small tip-sample separation, showing once a sudden jump (dashed lines),  $d_{ox}=0.9$  nm. (b)  $I$ - $V$  curves on a thicker oxide film ( $d_{ox}=1.8$  nm) and at larger tip-sample separation, measured between leakage sites (I) and on a leakage site (II). When ramping down the voltage, sometimes a transition from type II to type I is observed (indicated by III).

compared to the value around 1 eV we obtained from a rough estimate based on the measured low-bias resistance of our 0.7 nm oxide film and  $V_B = 1.2$  eV as obtained from ballistic electron emission microscopy (BEEM).<sup>12</sup> Thus, we believe that 1–1.5 eV is a reasonable estimate of the barrier height of our oxide film.

Regions of high and low conductance show a rather similar (nonlinear) shape of the  $I$ - $V$  curves, in agreement with earlier reports on soft breakdown.<sup>13</sup> For small tip-sample distances, however, the stability of the tunnel current during  $I$ - $V$  measurements was found to depend strongly on whether the tip was positioned on a highly conductive channel or in between such areas. Measured on a bright spot in the image, the  $I$ - $V$  curves are usually rather smooth. When measured on a low-conductive region between spots, abrupt and sizable jumps in the tunnel current are observed more often [Fig. 3(a)]. After such an event, a freshly created bright spot in the STM image can be found. For large tip-sample distances, i.e., limiting the current to  $< 100$  pA, the reverse process of a sudden and spontaneous decrease of the conductance can occur as shown by trace III in Fig. 3(b). While ramping down the voltage a sudden lowering of the conductance is observed corresponding to a transition from a curve characteristic for a high-conductive region (type II) to that of a low-conductive region (type I). This behavior corresponds to a reduced intensity of the leakage site in the corresponding STM image.

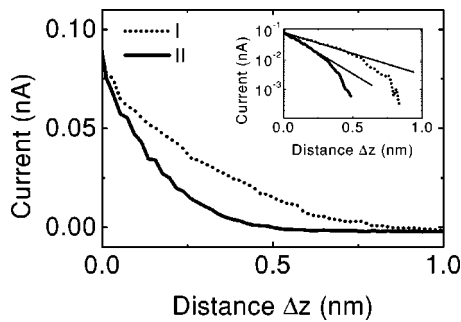


FIG. 4.  $I$ - $z$  spectroscopy, withdrawing the tip with feedback off and at  $V=3.3$  V, measured on (solid line) and off (dashed line) a leakage site,  $d_{ox}=1.8$  nm. The inset, with the same data, reveals the different initial slopes  $d\ln(I)/dz$ .

Differences between regions I and II are also visible in  $I$ - $z$  spectroscopy, i.e., varying the tip height with the STM feedback switched off. These  $I$ - $z$  characteristics provide an estimate of the effective barrier height, involving the work function of tip and sample.<sup>11</sup> In general, a higher work function gives rise to a faster decay of the current as a function of increasing tip-sample distance. Moreover, the decay rate is strongly influenced by a possible charging of the surface. Figure 4 resolves a clearly distinct  $I$ - $z$  dependence for different positions on the sample, with a low initial slope  $d\ln(I)/dz$  for region I and a higher slope for region II (see inset in Fig. 4).

The fact that the  $I$ - $z$  spectrum reveals different decay factors for measurements on and off a leakage site is an important indication that switching is accompanied by charge redistribution; for instance, trapped charge alters the image potential locally which results in a new barrierscape. It is known that trapped charge strongly affects the transport

properties of thin films.<sup>14,15</sup> Within this approach we can explain the switching behavior without requiring a metalliclike  $I$ - $V$  behavior after inducing a leakage site. Such a metallic behavior was observed by Da Costa *et al.*<sup>4</sup> and Magtoto *et al.*<sup>5</sup> and was attributed to dielectric (hard) breakdown. Our experiments show a nonlinear (nonmetallic) conductance at the leakage site, similar to observations by Watanabe *et al.* on silicon oxide films.<sup>7</sup> However, in our case a reversible behavior of the switching was observed, which may be considered as a precursor of the soft breakdown. Additionally, we like to add that the dimension of the leakage sites ( $\sim 2$  nm) is in excellent agreement with predictions by Oepts *et al.*,<sup>16</sup> who estimated a diameter of a few nanometers from macroscopic breakdown experiments.

In conclusion, we have studied the local current transport through  $\text{Al}_2\text{O}_3$  thin films identical to the ones used in MTJ's. A granular structure of the oxide is observed. We demonstrate the possibility to induce a reversible switching of leakage sites by injecting a high current density appearing in STM images, with an apparent height of 0.5–1 nm and a diameter of a few nanometers. While STS gave some insight into the underlying electronic processes, such as the role of charge redistribution, more detailed studies will be needed to fully unravel the switching phenomenon. The combination of different spectroscopic techniques, control of defects, and morphology of the oxide during deposition and oxidation, and a more careful study of the temperature dependence of the effects, will provide a more detailed understanding of the local transport through oxides and its manipulation.

This work forms part of the research program of the Dutch Foundation for Fundamental Research on Matter (FOM). P.LeC. is supported by the Dutch Technology Foundation STW.

<sup>1</sup>E. Miranda *et al.*, IEEE Trans. Electron Devices **47**, 82 (2000).

<sup>2</sup>J.S. Moodera and G. Mathon, J. Magn. Magn. Mater. **200**, 248 (1999).

<sup>3</sup>W. Oepts *et al.*, Appl. Phys. Lett. **73**, 2363 (1998).

<sup>4</sup>V. Da Costa *et al.*, Phys. Rev. Lett. **85**, 876 (2000).

<sup>5</sup>N.P. Magtoto *et al.*, Appl. Phys. Lett. **77**, 2228 (2000).

<sup>6</sup>H. Watanabe *et al.*, J. Appl. Phys. **85**, 6704 (1999).

<sup>7</sup>H. Watanabe *et al.*, Appl. Phys. Lett. **72**, 1987 (1998).

<sup>8</sup>P. LeClair *et al.*, Phys. Rev. Lett. **84**, 2933 (2000).

<sup>9</sup>P. LeClair *et al.*, J. Appl. Phys. **87**, 6070 (2000).

<sup>10</sup>R. Wiesendanger, *Scanning Probe Microscopy and Spectroscopy*

(Cambridge University Press, Cambridge, England, 1994), p. 637.

<sup>11</sup>Y. Kuk, in *Scanning Tunneling Microscopy*, edited by H.J. Güntherodt and R. Wiesendanger (Springer-Verlag, Berlin, 1992), p. 17.

<sup>12</sup>W.H. Rippard *et al.*, Appl. Phys. Lett. **78**, 1601 (2001).

<sup>13</sup>J. Suñé, G. Mura, and E. Miranda, IEEE Electron Device Lett. **167**, 167 (2000).

<sup>14</sup>R. Ludeke *et al.*, J. Vac. Sci. Technol. B **18**, 2153 (2000).

<sup>15</sup>J. Kolodzye *et al.*, IEEE Trans. Electron Devices **47**, 121 (2000).

<sup>16</sup>W. Oepts *et al.*, J. Appl. Phys. **86**, 3863 (1999).